

Adaptive Directional Total-Variation Model for Latent Fingerprint Segmentation

Jiangyang Zhang, Rongjie Lai, and C.-C. Jay Kuo, *Fellow, IEEE*

Abstract—A new image decomposition scheme, called the adaptive directional total variation (ADTV) model, is proposed to achieve effective segmentation and enhancement for latent fingerprint images in this work. The proposed model is inspired by the classical total variation models, but it differentiates itself by integrating two unique features of fingerprints; namely, scale and orientation. The proposed ADTV model decomposes a latent fingerprint image into two layers: cartoon and texture. The cartoon layer contains unwanted components (e.g., structured noise) while the texture layer mainly consists of the latent fingerprint. This cartoon-texture decomposition facilitates the process of segmentation, as the region of interest can be easily detected from the texture layer using traditional segmentation methods. The effectiveness of the proposed scheme is validated through experimental results on the entire NIST SD27 latent fingerprint database. The proposed scheme achieves accurate segmentation and enhancement results, leading to improved feature detection and latent matching performance.

Index Terms—Fingerprint recognition, fingerprint segmentation, latent fingerprints, total variation.

I. INTRODUCTION

LATENT fingerprint identification plays a critical role for law enforcement agencies in identifying and convicting criminals. An important step in an automated fingerprint identification systems (AFIS) is the process of fingerprint segmentation. Based on the collection procedure, fingerprint images can generally be divided into three categories, namely, *rolled*, *plain* and *latent* [1]. Rolled and plain prints are obtained in an attended mode so that they are usually of good visual quality and contain sufficient information for reliable matching. On the other hand, latent prints are usually collected from crime scenes and often mixed with other components such as structured noise or other fingerprints. Existing fingerprint recognition algorithms fail to work properly on latent fingerprint images, since they are mostly applicable under the assumption that the image is already properly segmented and there is no overlap between the target fingerprint and other components.

Manuscript received June 23, 2012; revised March 06, 2013 and May 09, 2013; accepted May 11, 2013. Date of publication June 10, 2013; date of current version July 02, 2013. The associate editor coordinating the review of this manuscript and approving it for publication was Prof. Alex Kot.

J. Zhang and C.-C. J. Kuo are with the Ming Hsieh Department of Electrical Engineering, University of Southern California, Los Angeles, CA 90089 USA (e-mail: cckuo@sipi.usc.edu; jiangyaz@usc.edu).

R. Lai is with the Department of Mathematics, University of Southern California, Los Angeles, CA 90089 USA (e-mail: rongjiel@usc.edu).

Color versions of one or more of the figures in this paper are available online at <http://ieeexplore.ieee.org>.

Digital Object Identifier 10.1109/TIFS.2013.2267491

Fingerprint segmentation refers to the process of decomposing a fingerprint image into two disjoint regions: foreground and background. The foreground, also called the region of interest (ROI), consists of the desired fingerprints while the background contains noisy and irrelevant contents that will be discarded in the following processing steps. Accurate fingerprint segmentation is critical as it affects the accurate extraction of minutiae and singular points, which are key features for fingerprint matching. When feature extraction algorithms are applied to a fingerprint image without segmentation, lots of false features may be extracted due to the presence of noisy background, and eventually leading to matching errors in the later stage. Therefore, the goal of fingerprint segmentation is to discard the background, reduce the number of false features, and thus improve matching accuracy.

Segmentation on rolled and plain fingerprint images has been well-studied in the literature. In the early work of [2], segmentation was achieved by partitioning a fingerprint image into blocks, followed by block classification based on gradient and variance information. This method was further extended to a composite method [3] that takes advantage of both the directional and variance approaches. Ratha *et al.* [4] considered the gray-scale variance along the direction orthogonal to the ridge-flow orientation as the key feature for block classification. In [5], fingerprints were segmented using three pixel-level features (i.e., coherence, mean and variance). An optimal linear classifier was trained for pixel-based classification and morphology operators were used to obtain compact segmentation clusters.

While significant efforts have been made in developing segmentation algorithms for rolled/plain fingerprints, latent fingerprint segmentation remains to be a challenging problem. Although automated identification has achieved high accuracy for plain/rolled fingerprints, manual intervention is still needed for latent prints processing [1]. The difficulty mainly lies in: 1) the poor quality of fingerprint patterns (in terms of the clarity of ridge information), and 2) the presence of various structured noise in the background. Traditional segmentation methods fail to work properly on latent fingerprints as they are based on many assumptions that are only valid for rolled/plain fingerprints. In recent work on latent fingerprints [6]–[8], the region-of-interest (ROI) is still manually marked and assumed to be known. Undoubtedly, accurate and robust latent segmentation is an essential step towards automatic latent identification, and it is the main focus of our current research.

Most recently, several studies [9]–[11] have been conducted to address the problem of latent fingerprint segmentation. Karimi-Ashtiani and Kuo [9] used a projection method to

estimate the orientation and frequency of local blocks. After projection, the distance between center-of-transient points measures the amount of data degradation and used for segmentation. Short *et al.* [10] formulated a ridge model template and used the cross-correlation between a local block and the generated template to assign one of six quality scores. Blocks with high quality score are labeled as the foreground while the rest are treated as the background. In [11], ridge orientation and frequency features were computed using the orientation tensor and local Fourier analysis, and the intersection of regions computed from both features is used to locate the latent fingerprint area. The effectiveness of their algorithm is validated through improved matching performance on two public latent fingerprint databases.

Fingerprint enhancement is the process of connecting broken ridges, separating joined ridges and removing overlapping patterns. In [8], a latent image is divided into blocks and short-time Fourier transform is first applied to obtain orientation hypothesis for each block. A randomized RANSAC procedure is used to evaluate each hypothesis and the Gabor filter is adopted to complete the final enhancement procedure. While experimental results demonstrated improved fingerprint matching accuracy, this approach still demands manual markups of the region-of-interest (ROI). Therefore, it would be desirable to have a solution that requires less human intervention, as it is crucial for automatic latent fingerprint identification.

Total-Variation-based (TV-based) image models have been widely used in the context of image decomposition [12], [13]. Among several well known TV-based models, the model using total variation regularization with an L1 fidelity term, denoted by the TV-L1 model, is especially suitable for multiscale image decomposition and feature selection [14], [15]. A modified TV-L1 model was adopted in [15] to extract small-scale facial features for facial recognition under varying illumination. More recently, the authors proposed an adaptive TV-L1 model for latent fingerprint segmentation in [16], where the fidelity weight coefficient is adaptively adjusted to the background noise level. Furthermore, the Directional Total Variation (DTV) model was formulated in [17] by imposing the directional information on the TV term, which proved to be effective for latent fingerprint detection and segmentation. It appears that the TV-based image model with proper adaptation offers a suitable tool for latent fingerprint segmentation. However, the performance of both models in [16], [17] was evaluated only subjectively, as no objective evaluation was performed to determine whether the proposed scheme improved matching accuracy, which is the ultimate goal for fingerprint segmentation.

In this paper, we take advantage of both TV methods in [16], [17] and combine them into one single model, called the Adaptive Directional Total Variation (ADTV) model. Both the anisotropic directional TV term and the spatially-adaptive fidelity weight are incorporated into the model formulation. The proposed ADTV model decomposes a latent fingerprint image into two layers: cartoon and texture. The cartoon layer contains the unwanted components (e.g., structured noise) while the texture layer mainly consists of the latent fingerprint. This cartoon-texture decomposition facilitates the segmentation process, as the region of interest can be easily detected from

the texture layer using traditional segmentation methods. In addition, our proposed solution is capable of completing two preprocessing tasks (i.e., segmentation and enhancement) at the same time, as it not only helps identify the latent fingerprint region but also enhances the ridges and valleys within the ROI. The effectiveness of our proposed scheme is validated through experiments on feature detection and latent matching. As compared with our prior work in [16], [17], the material in Sections III-C and IV is new. In Section III-C, we introduce the new ADTV model and propose the solution to this new model. In Section IV, we verify the effectiveness of our proposed solutions through experimental comparisons with other fingerprint segmentation algorithms and TV-based models.

The rest of this paper is organized as follows. In Section II, we examine several forms of structured noise that commonly appears in latent fingerprint images. In Section III, we introduce the proposed ADTV model and explain how it can be utilized for latent fingerprint image decomposition and segmentation. In Section IV, we validate the effectiveness of our proposed scheme through a series of benchmarking experiments. Concluding remarks are given in Section V.

II. STRUCTURED NOISE IN LATENT FINGERPRINT IMAGES

The difficulty for latent fingerprint segmentation mainly lies in two aspects. First, the fingerprint is usually of very poor quality, often with smudged or blurred ridges. It is common that the image contains only a partial fingerprint region, and large nonlinear distortions exist due to pressure variations. As a result, while a typical rolled fingerprint has around 80 minutiae, a latent fingerprint contains only about 15 usable minutiae with reasonable quality [1]. Second, the presence of various types of structured noise further hinders the proper segmentation for latent prints. As compared with the oscillatory ridge structures of fingerprints, structured noise is of much larger scale and can appear in various forms. Based on the appearance, structured noise can be classified into six categories: arch, line, character, speckle, stain and others. They are shown in Fig. 1 and elaborated below.

- 1) *Arch*. The big arch is manually marked by crime-scene investigators to indicate the possible existence of latent fingerprints in the region encircled by the arch. The arch noise is viewed as the simplest type of structured noise.
- 2) *Line*. The line noise may appear in form of a single line or multiple parallel lines. A single line is often detected and removed using methods based on the Hough transform [10]. Multiple parallel lines can be confused with fingerprints more easily since they share quite a few common features.
- 3) *Character*. This is one of the most common types of structured noise in latent fingerprints. Characters may appear in various font types, sizes and brightness. They can be either handwritten or typed.
- 4) *Stain*. It is generated when the fingerprint was inadvertently smeared on a wet or dirty surface. Stain noise often appears in spongy shape with inhomogeneous brightness.
- 5) *Speckle*. As compared with lines and characters, speckle noise tends to contain tiny-scale structures, which are ei-

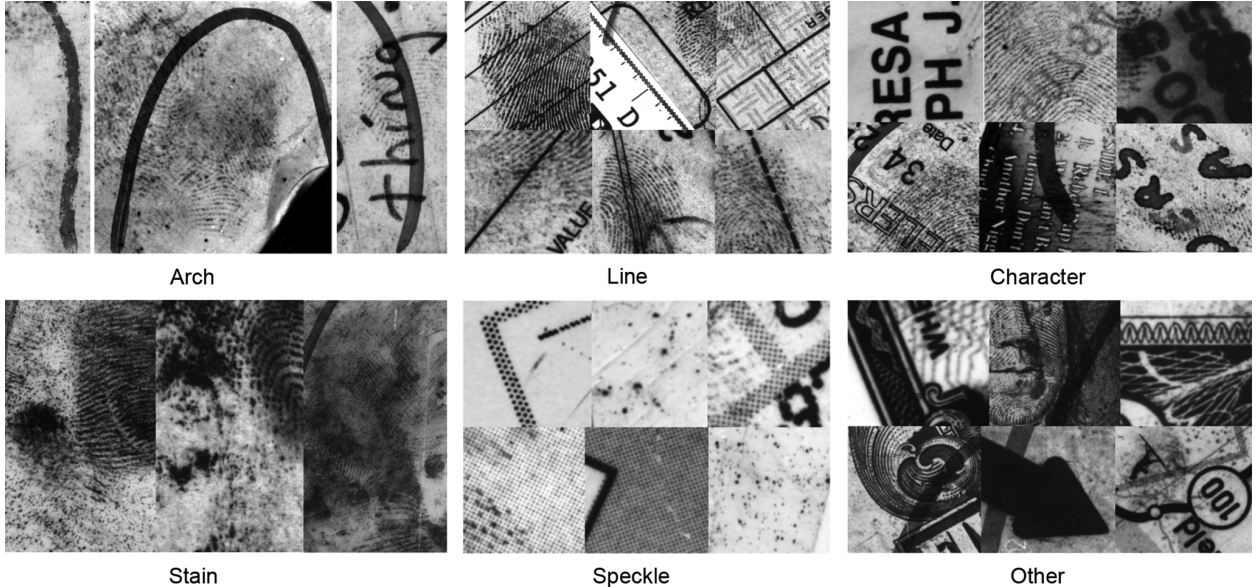


Fig. 1. Illustration of six types of structured noise in latent fingerprint images.

ther regular (e.g., clusters of small dots) or random (e.g., ink and dust speckles).

- 6) *Others*. A latent fingerprint may contain other types of structured noise such as arrows, signs, etc. Being similar to arch noise and character noise, they usually consist of smooth surfaces with sharp edges.

The line, character and speckle noise types often appear when the latent fingerprint is lifted from the surface of a text document (e.g., maps, newspapers, checks, etc.).

For latent fingerprint segmentation, the main challenge lies in how to effectively separate latent fingerprints, the relatively weak signal, from all structured noise in the background, which is often the dominant image component. Additional complexity arises when structured noise overlaps with the fingerprint signal. Previous methods proposed for fingerprint segmentation are mostly feature-based, and features commonly used for segmentation include the mean, variance, contrast, coherence as well as their variants [5], [18], [19]. However, these methods may fail to work properly for latent fingerprints as they are based on many assumptions that are only valid for rolled/plain fingerprints. For instance, in [5], the mean feature was used since the background was assumed to be bright and the variance feature was used since the variance of background noise was assumed to be much lower than that in fingerprint regions. However, these assumptions are no longer valid in the context of latent fingerprint images.

To evaluate the effectiveness of traditional segmentation features, we manually segment one plain and one latent fingerprint images, and plot the distributions of three segmentation features (namely, the mean, variance and coherence) for both foreground and background regions. As shown in Fig. 2, the distributions of these features in foreground and background regions are well separated for plain fingerprints while those of latent fingerprints have significant overlaps. These overlaps can be explained by two reasons. First, regions with structured noise often have high contrast and coherent gradient orientations as well that so it is difficult to differentiate them from fingerprints using these fea-

tures. Second, the quality of some latent fingerprints is so poor that they cannot be well characterized by traditional fingerprint features. As a result, new features or models need to be considered for more effective separation of latent fingerprint and structured noise.

III. LATENT SEGMENTATION WITH ADTV MODEL

In this section, we introduce the proposed Adaptive Directional Total Variation (ADTV) model and explain how it can be used to effectively separate the latent fingerprint from structured noise, thus facilitating the process of fingerprint segmentation. We begin with introducing the TV-L1 model, which serves as the basis for the proposed ADTV model, and then explain its capability in multiscale feature selection. Finally, we propose the ADTV model and discuss the choice of its parameters.

A. The TV-L1 Model

TV-based image models have been widely studied in the context of image decomposition. Among many existing TV models, the total variation regularization model with an L1 fidelity term, denoted by TV-L1, is suitable for multiscale image decomposition and feature selection. In the context of facial recognition under varying illumination, a modified TV-L1 model was proposed in [15] to separate small-scale facial features with nonuniform illumination to result in an improved recognition result.

Being similar to other TV-based image models (e.g., the ROF model [20]), the TV-L1 model decomposes an input image, f , into two signal layers:

- Cartoon u , which consists of the piecewise-smooth component in f , and
- Texture v , which contains the oscillatory or textured component in f .

The decomposition

$$f = u + v,$$

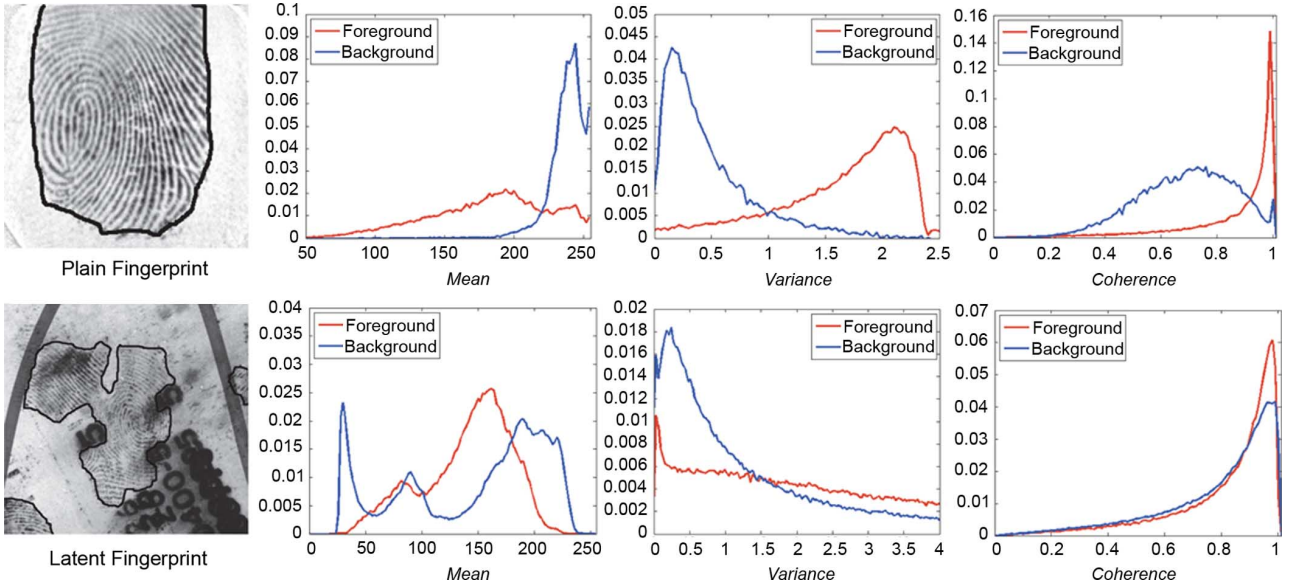


Fig. 2. Comparison of distributions of three features (mean, variance, and coherence) in the foreground and background areas of plain and latent fingerprints.

is obtained by solving the following variational problem:

$$\min_u \int |\nabla u| + \lambda \int |u - f| dx, \quad (1)$$

where f , u and v are functions of image gray-scale intensity values in \mathbb{R}^2 , ∇u is the gradient value of u and λ is a constant weighting parameter. We call $\int |\nabla u|$ and $\int |u - f|$ the total variation of u and the fidelity term, respectively.

The TV-L1 model is difficult to compute due to nonlinearity and nondifferentiability of the total variation term as well as the fidelity term. A gradient descent approach was proposed in [14], which solves for u as a steady solution to the following Euler-Lagrange equation with respect to the optimization problem in (1):

$$\nabla \cdot \left(\frac{\nabla u}{|\nabla u|} \right) + \lambda \frac{f - u}{|f - u|} = 0. \quad (2)$$

Although Equation (2) is easier to solve numerically, the gradient descent approach is slow due to a small time step imposed by the strict stability constraint. That is, the term $f - u / |f - u|$ is nonsmooth at $f - u$, which forces the time step to be very small when the solution is approaching the steady state. In addition, $|\nabla u|$ in the term $\nabla u / |\nabla u|$ might be zero, and a small positive constant needs to be added to avoid zero division, which results in an inexact solution.

Many numerical methods have been proposed to improve this method. One approach is the split Bregman iteration [21]–[24], which uses functional splitting and the Bregman iteration for constrained optimization. The equivalence of the split Bregman iteration to the alternating direction method of multipliers (ADMM), the Douglas-Rachford splitting, and the augmented Lagrangian method can be found in [24]–[27].

The use of the TV model is motivated by the analogy between the problem of TV decomposition and latent fingerprint segmentation. As discussed in Section II, the key challenge for latent segmentation is to effectively separate the underlying latent fingerprint from various structured noise. Structured noise

with its smooth inner surface and crisp edges has many similar characteristics with components in cartoon layer u . On the other hand, a fingerprint pattern, which consists of oscillatory ridge structures, matches the characteristics of texture components in v . This interesting analogy suggests that the TV model could be a viable solution to the challenging latent fingerprint segmentation problem.

B. Multiscale Feature Selection of TV Model

The TV-L1 model distinguishes itself from other TV-based models by its unique capability of intensity-independent multiscale decomposition. It was shown theoretically [14] as well as experimentally [12] that the fidelity weight coefficient, λ , in (1) is closely related to the scale of features in texture output v . This relation is supported by an analytic example in [14]. That is, if f is a disk signal denoted by B_r , which has radius r and unit height, the solution to the minimization problem in Equation (1) is given by

$$u_\lambda(x) = \begin{cases} 0 & \text{if } 0 \leq \lambda < \frac{2}{r} \\ f(x) & \text{if } \lambda > \frac{2}{r} \\ cf(x) & \text{if } \lambda = \frac{2}{r}, \text{ for any } c \in [0, 1] \end{cases}.$$

In other words, depending on the λ value, the TV-L1 functional is minimized by either 0 or input f . This shows that the TV-L1 model has the ability to select geometric features based on a given scale. Fig. 3 shows an example of feature selection from a latent fingerprint image.

As shown in Fig. 3, the numerical result matches the analytical one well. The fidelity weight coefficient, λ , controls the feature selection process by manipulating the scale of contents captured in each image layer. When λ is very small (e.g., $\lambda = 0.10$), u captures the inhomogeneous illumination in the background while most fine structures are kept in v . When $\lambda = 0.30$, large-scale objects (arch) are captured in u but separated from structures of smaller scales (characters). As λ continues to increase, only small-scale structures (fingerprint and noise) are left in v while the major content of f is extracted to u .

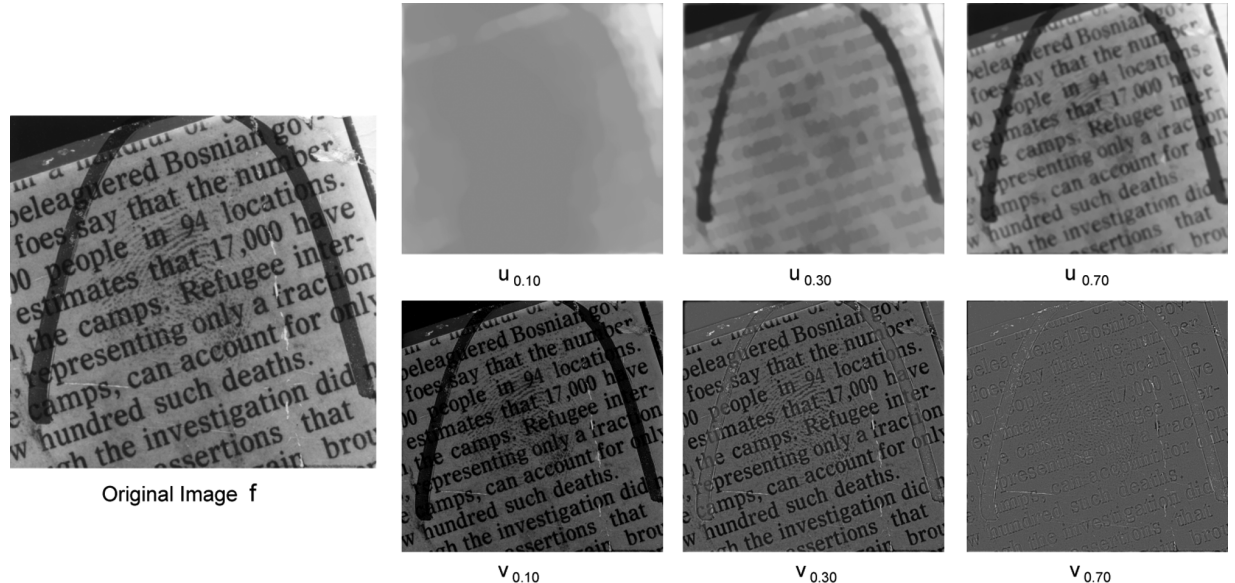


Fig. 3. Feature selection based on the TV-L1 model for a latent fingerprint image: input image f (left most) and its TV-L1 decomposed components u and v with its λ value shown in the subscript. As λ increases, only features of smaller scales are extracted to texture output v while features of larger scales are kept in cartoon u .

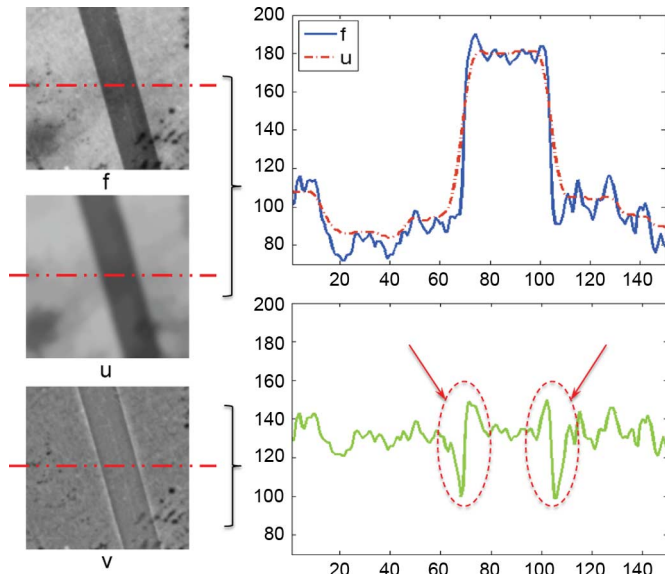


Fig. 4. Illustration of the boundary signal problem in TV-L1 decomposition: a small amount of structure noise edge signal is still kept in texture v (left) and signals along the dashed line depicted in f , u , and v (right).

We observe that one of the differences between fingerprint patterns and structure noise is their relative scale. By applying the TV-L1 model with an appropriately chosen λ value, it is seemingly possible to extract fingerprints to texture layer v while leaving the unwanted structure noise in cartoon layer u . However, there arise two problems by applying the TV-L1 model directly.

- 1) The value of λ forces structures that are smaller or equal to a given scale to appear in v . As a result, structured noise of smaller scales as fingerprints (e.g., speckle, stain) will be captured by v along with fingerprints.
- 2) A small amount of boundary signals near nonsmooth edges will appear in v (see Fig. 4) due to the nonsmoothness of

the boundary and the use of finite differencing. This issue was also reported in [15].

To overcome these limitations, we propose an Adaptive Directional Total-Variation (ADTV) model in the next subsection.

C. The ADTV Model

The TV-L1 model with spatially invariant fidelity (1) does not generate the desired output throughout the entire fingerprint image. In the fingerprint region, when λ is well matched with the scale of fingerprints, all essential contents can be captured in texture layer v . However, in the noisy region, some unwanted signals will be extracted to v under the same λ value. In addition, being an isotropic model, the TV model minimizes the total variation of cartoon layer u along all directions. This scheme does not fully exploit the orientation coherency, which is one of the most unique characteristics of fingerprints. These observations motivate us to study a more flexible image model that is capable of integrating the special characteristics of fingerprints. It is called the Adaptive Directional Total-Variation (ADTV) model and formulated as

$$u^* = \operatorname{argmin}_u \int |\nabla u \cdot \vec{a}(x)| dx + \frac{1}{2} \int \lambda(x) |u - f| dx, \quad (3)$$

where $\vec{a}(x)$ is a spatially varying orientation vector adjusted by the local texture orientation, and $\lambda(x)$ is a spatially varying parameters that controls the feature scale.

The spatially varying parameter, $\lambda(x)$, can be understood in two ways. First, $\lambda(x)$ is a scalar that controls the scale of features appearing in v at pixel x . A large $\lambda(x)$ value enforces most textures to be kept in u , leaving only tiny-scale structures in v . When $\lambda(x)$ is sufficiently large, $u^*(x) \approx f(x)$, and the original content is almost totally blocked from v . Thus, $v(x) = f(x) - u^*(x) \approx 0$. Second, parameter $\lambda(x)$ can be interpreted as a weighting coefficient that balances the importance between fidelity and smoothness of u . In the fingerprint region,

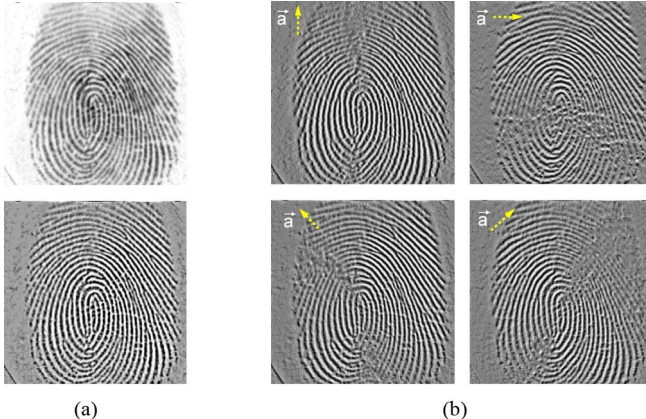


Fig. 5. (a) Top: original image f . Bottom: texture output v after decomposition by the TV-L2 model [20]. (b) Texture output v for orientation vector \vec{a} in four different directions. Top: $\vec{a} = (0, 1)$ and $\vec{a} = (1, 0)$. Bottom: $\vec{a} = (-\sqrt{2}/2, \sqrt{2}/2)$ and $\vec{a} = (\sqrt{2}/2, \sqrt{2}/2)$.

the $\lambda(x)$ value should be relatively small since low fidelity ensures the smoothness of u and, thus, more textures will go to v . In regions with structured noise, fidelity becomes important and a large $\lambda(x)$ value ensures all noise components to be filtered out from texture v .

The orientation vector, $\vec{a}(x)$, also controls the content captured in the texture layer v but in a different manner. By tuning $\vec{a}(x)$ to a specific direction, we are mainly interested in minimizing the total variation of u along that direction while allowing the variation of u to exist along other directions. As a result, textures along the corresponding direction will be fully captured by v while textures of other directions will be weakened in v . In particular, textures along the orthogonal direction of $\vec{a}(x)$ will be totally blocked from v . In Fig. 5, we illustrate the impact of $\vec{a}(x)$ on the texture output v by applying the ADTV model with fixed orientation vector \vec{a} on a typical fingerprint image. In the proposed ADTV model, $\vec{a}(x)$ is a spatially varying vector that is adaptively chosen according to the image content.

Algorithm 1. Augmented Lagrangian method for our proposed ADTV model.

- 1) *Initialization:* $u^0 = 0, \vec{p}^0 = 0, q^0 = 0, w^0 = 0;$
- 2) For $k = 0, 1, 2, \dots$, compute:

$$(u^{k+1}, \vec{p}^{k+1}, q^{k+1}, w^{k+1}) = \underset{(\vec{u}, \vec{p}, q, w)}{\operatorname{argmin}} \mathcal{L}(u, \vec{p}, q, w, \mu_p^k, \mu_q^k, \mu_w^k). \quad (4)$$

- 3) *Update:*

$$\begin{aligned} \vec{\mu}_p^{k+1} &= \vec{\mu}_p^k + r_p(\vec{p}^{k+1} - \nabla u^{k+1}) \\ \mu_q^{k+1} &= \mu_q^k + r_q(q^{k+1} - \vec{p}^{k+1} \cdot \vec{a}) \\ \mu_w^{k+1} &= \mu_w^k + r_w(w^{k+1} - u^{k+1}). \end{aligned}$$

We use the augmented Lagrangian method [28]–[31] to solve the proposed ADTV model given in Equation (3). The augmented Lagrangian method is both accurate and efficient, as it benefits from the FFT-based fast solver with a closed-form

solution. It has been proven that the augmented Lagrangian is equivalent to the split Bregman iteration and its convergence is always guaranteed [24].

In the augmented Lagrangian method, three new variables, \vec{p}, q , and w , are introduced to reformulate (3) into the following constraint optimization problem:

$$\begin{aligned} \min_u \quad & \int |q| + \frac{1}{2} \int \lambda(x) |w - f| dx, \\ \text{s.t.} \quad & \vec{p} = \begin{pmatrix} p_1 \\ p_2 \end{pmatrix} = \begin{pmatrix} \partial_x u \\ \partial_y u \end{pmatrix} = \nabla u, q = \vec{p} \cdot \vec{a}, w = u. \end{aligned} \quad (5)$$

To solve (5), the following augmented Lagrangian functional is defined:

$$\begin{aligned} \mathcal{L}(u, \vec{p}, q, w, \mu_p, \mu_q, \mu_w) = & \int |q| + \frac{1}{2} \int \lambda(x) |w - f| dx \\ & + \frac{r_p}{2} \int (\vec{p} - \nabla u)^2 + \int \mu_p (\vec{p} - \nabla u) \\ & + \frac{r_q}{2} \int (q - \vec{p} \cdot \vec{a})^2 \\ & + \int \mu_q (q - \vec{p} \cdot \vec{a}) \\ & + \frac{r_w}{2} \int (w - u)^2 + \int \mu_w (w - u), \end{aligned}$$

where $\vec{\mu}_p, \mu_q$ and μ_w are the Lagrange multipliers and r_p, r_q and r_w are positive constants. The augmented Lagrangian method uses an iterative procedure to solve (5) as shown in Algorithm 1. The iterative scheme runs until some stopping condition is met. Since variables u, \vec{p}, q, w in $\mathcal{L}(u, \vec{p}, q, w, \mu_p, \mu_q, \mu_w)$ are coupled together, it is difficult to solve them simultaneously. Instead, the problem is decomposed into four subproblems and an alternative minimization process is applied. Instead of solving (4) exactly, we apply the alternating direction method of multipliers (ADMM) [24], [25] and run one iteration for each subproblem. It should be mentioned that this was also reused in the split Bregman iteration method [26], [27]. This approach of splitting technique is efficient since all subproblems have closed-form solutions; namely,

$$\begin{aligned} u^k &= \mathcal{F}^{-1} \left(\frac{-r_p \cdot \mathcal{F}(\operatorname{div} \cdot \vec{p}) - \mathcal{F}(\operatorname{div} \cdot \vec{\mu}_p^k) + r_w \mathcal{F}(w) + \mathcal{F}(\mu_w^k)}{r_w - r_p \mathcal{F}(\Delta)} \right), \\ \vec{p}^k(x) &= \nabla u - \frac{1}{r_p} \left(\vec{\mu}_p^k - (r_q q - r_q \rho(x) + \mu_q^k) \cdot \vec{a}(x) \right), \\ q^k(x) &= \max \left\{ 0, 1 - \frac{1}{r_q |\psi(x)|} \right\} \cdot \psi(x), \\ w^k(x) &= \max \left\{ 0, 1 - \frac{\lambda(x)}{r_w |\phi(x)|} \right\} \cdot \phi(x) + f(x) \end{aligned}$$

where $\rho(x) = r_p(\nabla u \cdot \vec{a}(x)) - \vec{\mu}_p^k \cdot \vec{a}(x) + (\mu_q^k + r_q q) \|\vec{a}(x)\|^2 / r_p + r_q \|\vec{a}(x)\|^2, \psi(x) = \vec{p} \cdot \vec{a}(x) - \mu_q^k(x) / r_q$, and $\phi(x) = u(x) - f(x) - \mu_w^k(x) / r_w$. Furthermore, $\mathcal{F}(u)$ and $\mathcal{F}^{-1}(u)$ denote the Fourier transform and inverse Fourier transform of u , respectively.

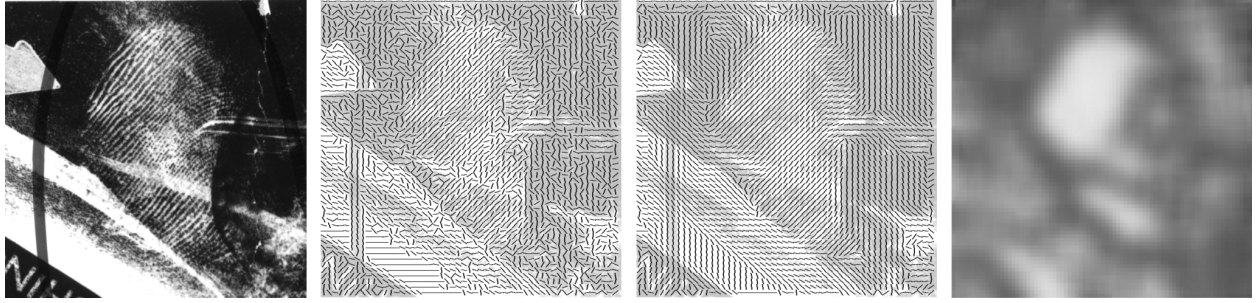


Fig. 6. Essential steps in the computation of $\vec{a}(x)$ (from left to right): original image f , coarse orientation estimation $o(x)$, orientation smoothening $O(x)$, and coherency evaluation $c(x)$.

D. Orientation Field Estimation

In order to extract the fingerprint components to texture output v , $\vec{a}(x)$ should be spatially varying and well aligned with the local fingerprint ridge orientation. We use the gradient-based approach [32], [33] to compute the coarse orientation field at each pixel:

$$o(x) = \frac{1}{2} \tan^{-1} \frac{\sum_W 2f_{x_1} f_{x_2}}{\sum_W (f_{x_1}^2 - f_{x_2}^2)} + \frac{\pi}{2}, \quad (6)$$

where W is a neighborhood window around x , (f_{x_1}, f_{x_2}) is the gradient vector at $x = (x_1, x_2)$, and \tan^{-1} is a 4-quadrant arctangent function with output range of $(-\pi, \pi)$. The estimation given above is relatively accurate at fingerprint regions, while it becomes less reliable at noisy regions. We evaluate the reliability of the estimated orientation field by its local coherency:

$$c(x) = \frac{(\sum_W (f_{x_1}^2 - f_{x_2}^2))^2 + 4(\sum_W f_{x_1} f_{x_2})^2}{(\sum_W (f_{x_1}^2 + f_{x_2}^2))^2}, \quad (7)$$

where $c(x) \in [0, 1]$ (close to 1 for strongly oriented pattern, and 0 for isotropic regions). The value of $c(x)$ provides a reliability measure of the estimated orientation field and will be utilized to generate the final orientation vector, $\vec{a}(x)$.

The coarse orientation field $o(x)$ still contains inconsistencies caused by creases and ridge breaks of the fingerprint pattern. We further improve the estimation by orientation smoothening:

$$O(x) = \frac{1}{2} \tan^{-1} \left\{ \frac{G_\sigma * \sin(2 \cdot o(x))}{G_\sigma * \cos(2 \cdot o(x))} \right\}, \quad (8)$$

where G_σ is a Gaussian smoothing kernel with standard deviation σ . Finally, the orientation vector $\vec{a}(x)$ in (3) is computed as

$$\vec{a}(x) = (-\cos O(x), \sin O(x)) \cdot c(x). \quad (9)$$

The process for computing $\vec{a}(x)$ is illustrated by an example in Fig. 6.

At regions where the orientation estimation is reliable, the large $c(x)$ value enforces textures along the direction of $\vec{a}(x)$ to be fully captured by v , leaving textures of other orientations in u . On the other hand, at regions where $c(x)$ is small and the estimation is not trustworthy, the fidelity term $1/2 \int \lambda(x) |u - f| dx$ becomes dominant and most of the image content will be kept in u . In this way, we can efficiently filter out structured noise from texture output v .

E. Scale Parameter Selection

As discussed in Section III-B, applying one uniform λ value over the entire fingerprint image does not generate satisfactory results. To improve the result, the value of λ should be spatially adaptive. That is, $\lambda(x)$ ought to be adaptively chosen according to the background noise level. Ideally, parameter $\lambda(x)$ should be larger in regions with higher structured noise and smaller in fingerprint regions.

To differentiate these regions, we study their characteristics after going through local low-pass filtering. When an input image, f , is locally filtered by a low-pass filter denoted by

$$L_\sigma(\xi) = \frac{1}{1 + (2\pi\sigma|\xi|)^4}, \quad (10)$$

its cartoon and texture components, although both being blurred to some extent, change differently in their individual local total variation (LTV), which is defined as

$$LTV(f) = G_\sigma * |\nabla f|, \quad (11)$$

where f is the image region and G_σ is a Gaussian kernel with standard deviation σ . In [34], the relative LTV reduction ratio is used to differentiate the cartoon region from the textural region. It was observed that the LTV of textural regions decay much rapidly than that of cartoon regions after low-pass filtering.

Although the LTV reduction ratio provides a good measure for separating edgy regions from textural regions, it has limited capability in differentiating textures of different scales (e.g., fingerprints with speckles). To overcome this limitation, we further introduce the differential LTV reduction rate as

$$\eta_\sigma = \frac{LTV(L_{\sigma+1} * f) - LTV(L_\sigma * f)}{LTV(f)}. \quad (12)$$

For a given local patch, parameter η_σ describes its structural component's sensitivity to low-pass filtering of scale σ , and provides useful information about the underlying textural structure of a local region. Intuitively, it measures texture's local oscillatory behavior at a certain spatial scale σ .

We show the η_σ values of different textural patches, which are extracted from latent fingerprint images, in Fig. 7. The η_σ value of fingerprint regions all reaches local maxima around $\sigma = 2.0$. For a given σ value, η_σ will have the largest response for texture of scale around σ while the response for texture of other scales is suppressed.

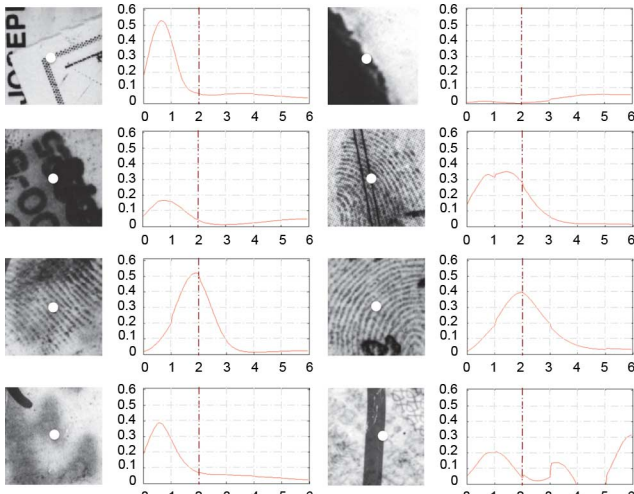


Fig. 7. Plots of $\eta_\sigma(x)$ for several pixels in different latent fingerprint images. It has a sharp peak located near $\sigma = 2.0$ in the fingerprint region while it reaches the maximum at different σ values in other regions.

Based on this observation, we choose the spatially variant coefficient $\lambda(x)$ in (3) as

$$\lambda(x) = \kappa \cdot \frac{1}{\eta_c(x) + \epsilon}, \quad (13)$$

where η_c is the differential LTV reduction rate at $\sigma = c$, which is adjusted to the best response of fingerprint patterns, κ and ϵ are trivial positive constants used for scaling and avoiding zero-division. In our experiments, we observe that $c = 2.0$ gives the optimum value for the latent fingerprint pattern while parameters κ and ϵ are empirically set to 0.5 and 0.01, and used for scaling and avoiding zero-division, respectively.

F. Region-of-Interest Segmentation and Enhancement

After decomposing the latent fingerprint image using the proposed ADTV model, we obtain two image layers: 1) cartoon u , which contains the majority of unwanted content (e.g., structured noise, small-scale structures), and 2) texture v , which consists of latent fingerprints and only a small amount of random noise. This decomposition facilitates two procedures: segmentation and enhancement. The variance value acts as a key segmentation feature for rolled/plain fingerprints [5]. As discussed in Section II, this feature cannot be directly applied to latent fingerprints due to the presence of structured noise. However, after the cartoon-texture layer decomposition, most high-variance noise components are kept away from texture layer v , allowing us to use the variance features for segmentation. As shown in Fig. 8, the variance distributions of foreground/background regions are more widely separated after the ADTV-based decomposition, making it possible to conduct segmentation by simple variance-based block classification.

In addition, the proposed decomposition scheme is capable of enhancing the fingerprint quality. After decomposition, we remove all unwanted components that may overlap with fingerprints in texture layer v . The extracted patterns are less degraded by structured noise and free from the illumination effect, leading to enhanced fingerprint quality. In the next section, we will demonstrate that the enhancement and segmentation task will result in better latent matching performance experimentally.

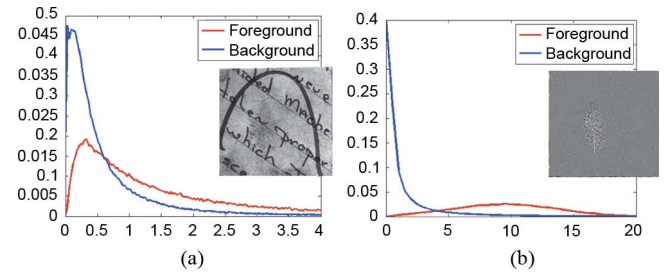


Fig. 8. Distributions of the variance feature for the foreground and background region in f and v , respectively. (a) Input f ; (b) Texture v .

TABLE I
COMPUTATIONAL TIME FOR THE PROPOSED ADTV-BASED LATENT FINGERPRINT SEGMENTATION ALGORITHM

Procedure	Time (sec)
Generate λ map	2.35
Generate orientation map	0.33
ADTV Decomposition (150 iterations)	100.33
ROI Segmentation	4.01
Total	107.02

IV. EXPERIMENTAL RESULTS

In this section, we evaluate the proposed ADTV model through a series of experiments. We first show the segmentation results for latent fingerprint images with different quality types. We compare our results with two segmentation approaches [5], [11]. The approach in [5] uses a linear-classifier for conducting segmentation on rolled fingerprints, while [11] was designed specifically for latent segmentation. Then, we experimentally examine the impact of our proposed segmentation scheme on the accuracy of feature extractions. We also conduct latent matching experiments to verify whether the segmentation result can indeed lead to higher matching accuracy. Finally, we compare the performance of our proposed ADTV model with two other TV-based models: the TV-L1 [14] and TVL2 [20] model. The algorithm was implemented on a MacBook Pro computer with 2.3 GHz Intel Core i7. For a 1000ppi latent fingerprint image of size 1131×1321 , the computational time of each procedure is listed in Table I.

A. Results of Good, bad and Ugly Fingerprint Processing

All experiments were conducted on the public domain latent fingerprint database, NIST SD27, which contains 258 latent fingerprints and their corresponding rolled fingerprints. In this database, fingerprint experts have assigned to each fingerprint one of three quality levels—good, bad and ugly. The numbers of good, bad and ugly latent prints are 88, 85 and 85, respectively. For the fingerprint matching experiments (Sections IV-D and IV-E), we included 27,000 rolled fingerprints from the NIST SD14 database [35] and extended the background database to 27,258 fingerprints, making the problem more realistic and challenging.

We ran the proposed algorithm over the entire NIST SD-27 database [36], and put all results in the supplemental material that goes with this work. Furthermore, we have also uploaded the same results online [37] so that other researchers can use it to make fair comparison in the future. The processing results of using the proposed ADTV model for three good, two bad and

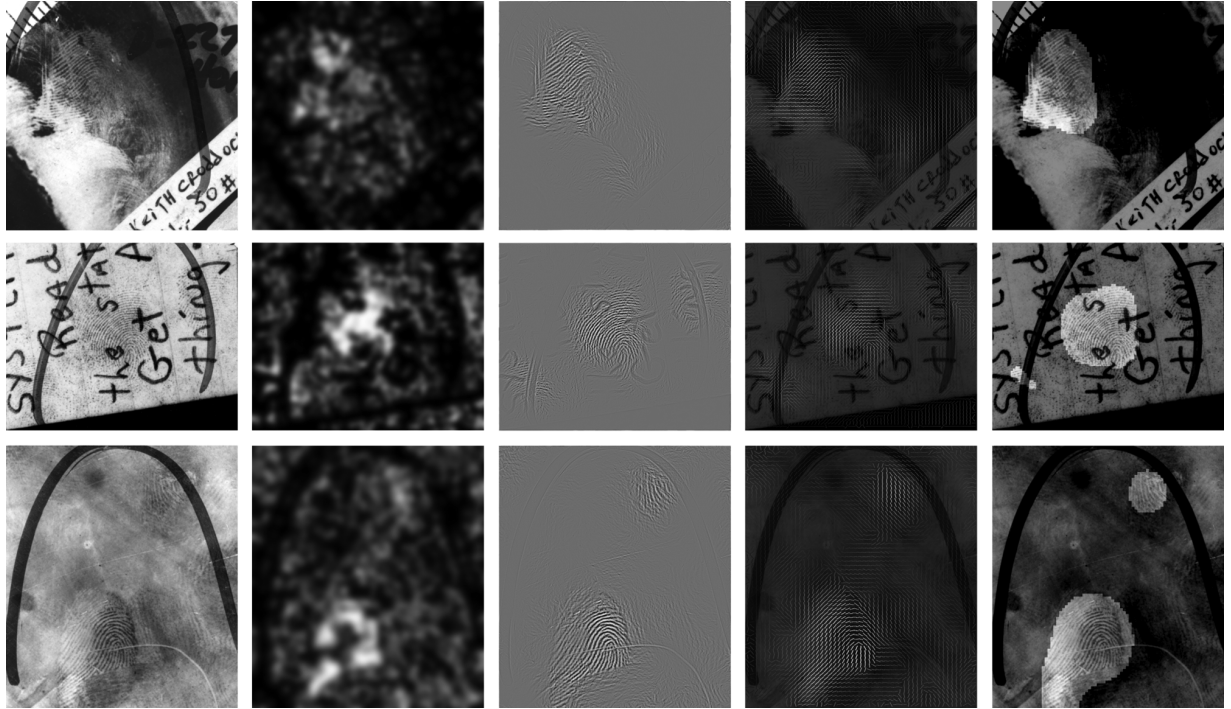


Fig. 9. Experimental results of three latent fingerprints with *good* quality (from left to right): original image f , scale parameter $\lambda(x)$, texture output v , orientation vector $\vec{d}(x)$, and the final segmentation result.

two ugly representative latent fingerprints are shown in Figs. 9, 14 and 15, respectively.

Visual inspection shows that the proposed ADTV scheme provides satisfactory results, as the most essential fingerprint regions lie within the segmented foreground. It should be noted that it is difficult for the proposed decomposition scheme to perfectly erase structure noise from the texture layer v . For instance, in Figs. 9, some part of the characters can still be observed in v . The goal of ADTV decomposition is to suppress the structure noise components from texture layer v as much as possible so that the region-of-interest can be more easily identified using the variance feature.

B. Comparison With Other Segmentation Methods

We first compare the segmentation accuracy of our approach with two other fingerprint segmentation methods: the linear-classifier-based approach [5] and the latent segmentation approach [11]. The segmentation accuracy is evaluated using two measures: the Missed Detection Rate (MDR) and the False Detection Rate (FDR) [11]. We use the manual segmentation results provided by [36] as the ground truth. MDR is defined as the average percentage of foreground pixels misclassified as background, while FDR refers to the average percentage of background pixels misclassified as foreground. The average segmentation accuracy of the proposed approach and the other two segmentation methods for the entire NIST SD27 database is shown in Table II.

While the linear classifier approach [5] works well on segmenting rolled fingerprints, it performs poorly on latent images. Although its MDR is relatively low (around 5%), its FDR is much higher than [11] and our approach because much of the background structure noise region is mistakenly classified as foreground. As compared with the approach by Choi *et al.* [11],

TABLE II
PERFORMANCE COMPARISON OF THREE SEGMENTATION ALGORITHMS

Segmentation algorithm	MDR (%)	FDR (%)
Bazen <i>et al.</i> [6]	5.04	79.31
Choi <i>et al.</i> [12]	14.78	47.99
Our approach	14.10	26.13

while the two segmentation methods have about the same level of MDR, the FDR of our proposed method is about 20% lower.

C. Feature Extraction Accuracy

Without segmentation, the performance of latent matching is very poor due to the high number of unreliable features. There are two types of features that are essential to fingerprint matching: singular points (SPs) and minutiae. Traditional feature extraction algorithms perform poorly on latent fingerprints, especially at regions with much structured noise. Some areas of noise are often miss-identified as useful fingerprint features, which can affect the accuracy of the fingerprint matching stage significantly. Thus, with the help of accurate segmentation, we can remove unwanted structured noise components and, therefore, decrease the number of erroneous features.

Again, we use the manual segmentation results of [36] as the ground truth, and use VeriFinger SDK 6.6 [38] for feature extraction. All extracted features points that fall within the manual segmentation region are used as the ground truth. Then, we calculate the number of true features points that were missing and the number of false feature points detected for two scenarios (with and without ADTV-based segmentation). For cases without segmentation, we conduct feature extraction directly on the original image (Type-1 input) while, for cases with segmentation, feature extraction was conducted on our segmentation results (Type-2 input).

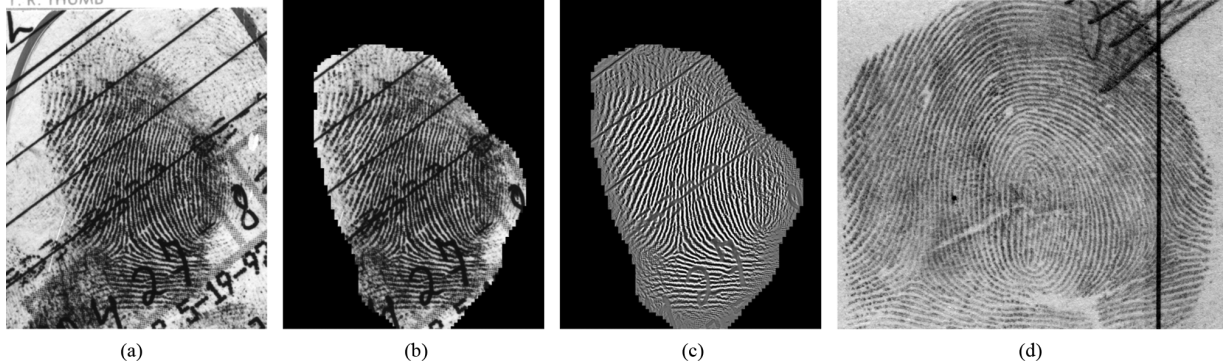


Fig. 10. Three input image types for latent matching. (a) Type-1: without any segmentation; (b) Type-2: segmentation mask over original image f ; (c) Type-3: segmentation mask over texture layer v ; (d) the corresponding mated rolled fingerprint. (a) Latent print input: Type-1. (b) Latent print input: Type-2. (c) Latent print input: Type-3. (d) Mated rolled fingerprint.

TABLE III
FEATURE EXTRACTION ACCURACY WITH AND WITHOUT ADTV-BASED SEGMENTATION

	w.o. segmentation	w. segmentation
Missed Minutiae	0.0%	3.23%
Missed SPs	0.0%	3.32%
False Minutiae	73.69%	31.52%
False SPs	71.47%	30.73%

Experimental results are given in Table III. For latent inputs without any segmentation, though none of true features points are missing, more than 70% of the detected features are erroneous as many incorrect feature points were detected in the structure noise regions. On the other hand, for inputs with our ADTV segmentation, the false feature point ratio has decreased to around 30% while the missing features points have only slightly increased by 3%. In the next subsection, we will show that the improvement in feature extraction will lead to better matching performance.

D. Fingerprint Matching Results

The ultimate goal of segmentation is to successfully match the input latent fingerprint with the corresponding plain/rolled fingerprint in a large database. and shown that the segmentation does improve the accuracy of feature extractions. In this subsection, we conduct matching experiment to verify whether the segmentation result can indeed lead to improved matching accuracy.

The feature extraction and fingerprint matching process are conducted using the commercial matcher Neurotechnology VeriFinger SDK 6.6 [38]. For each latent fingerprint, we compare the results for three input types:

- Type-1: original latent fingerprint without segmentation,
- Type-2: segmentation mask applied on original image,
- Type-3: segmentation mask applied on texture layer v .

An example of the three input image types is given in Fig. 10. As mentioned earlier, the proposed ADTV model has two functionalities: segmentation and texture enhancement. We can evaluate the effectiveness of segmentation by comparing the corresponding results of Type-1 and Type-2 images and the impact of texture enhancement by comparing the matching results of Type-2 and Type-3 images.

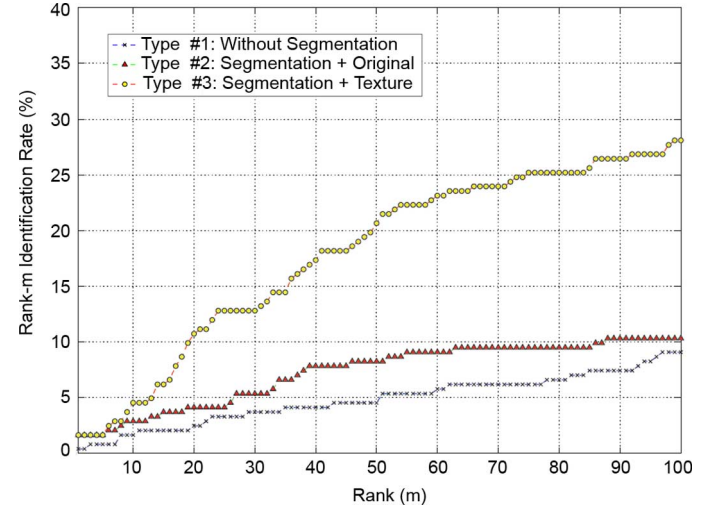


Fig. 11. Cumulative matching curves (CMC) of all three latent fingerprint input types for good-quality latent fingerprints.

The Cumulative Match Characteristic (CMC) curves of the three input types to the fingerprint matcher are shown in Fig. 11. Each input is searched against the background database of 27,258 rolled fingerprint from both NIST SD27 and NIST SD14 database. The CMC curve plots the rank- k identification rate against $k = 1, 2, 3, \dots, 100$. As shown in Fig. 11, automatic matching performance is significantly improved when Type-2 and Type-3 are used as the input to the matcher. The rank-20 identification ratio has increased from 2.48% (Type-1) to 4.13% (Type-2) and 10.74% (Type-3).

E. Comparison With Other TV-Based Models

In Fig. 12, we compare the texture output v of the proposed ADTV model with two classical TV models: TV-L1[14] and TV-L2 [20]. The variance distribution of foreground/background regions as well as the corresponding segmentation result are shown in the bottom part of Fig. 12, respectively. In fingerprint regions, the proposed ADTV model is able to extract all essential fingerprint texture with clear ridge information, while the results of other TV models still contain some background noise. In regions with structured noise, boundary and speckle noise can be clearly observed in the texture layer, v , obtained by other TV-based models. In contrast, the proposed

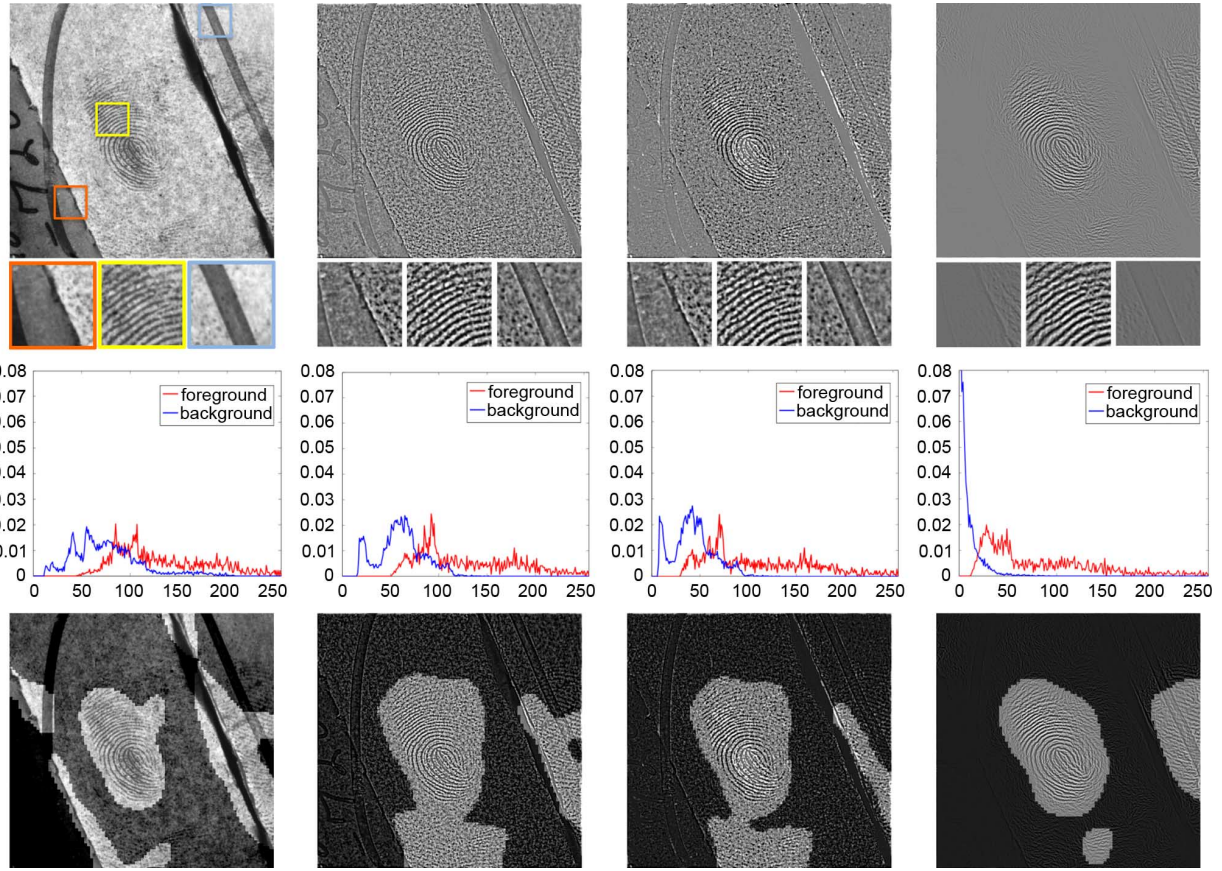


Fig. 12. Performance comparison of the proposed ADTV model and two other TV-based models. First row: original image f , texture output v of TV-L2 [20], TVL1 [14] and the proposed ADTV model (from left to right). Second row: distribution of variance feature in the foreground and background areas. Third row: the segmentation result based on variance feature.

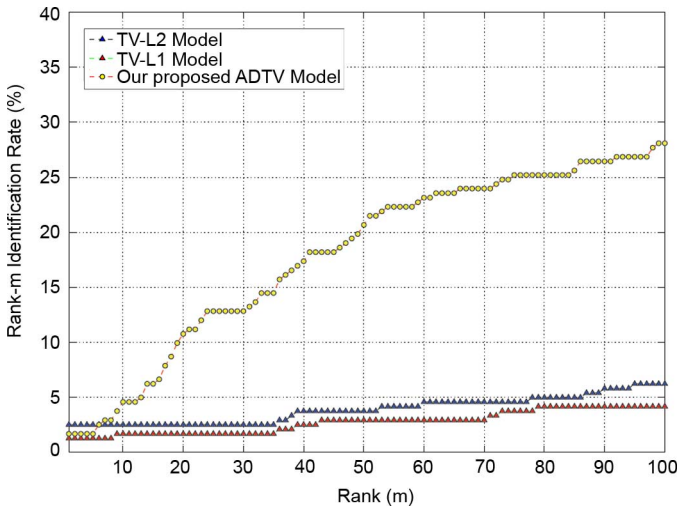


Fig. 13. Comparison of the cumulative matching curves (CMC) of the proposed ADTV model and two other TV-based models.

ADTV model can filter out the background noise signals from texture output v .

The CMC curves of two TV-based models and the proposed ADTV model are shown in Fig. 13, where we show the Type-3 result (segmentation + texture) of each TV model to match against the same background database. As shown in Fig. 13, the proposed ADTV model offers significantly better matching

performance and its rank-20 identification ratio is about 5 times higher than the TV-L1 and the TV-L2 models.

V. CONCLUSION AND FUTURE WORK

While current automated fingerprint identification systems have achieved high accuracy in matching rolled/plain prints, latent fingerprint matching remains to be a challenging problem and requires much human intervention. The goal of this work is to achieve accurate latent segmentation, which is an essential step towards automatic latent identification. Existing fingerprint segmentation algorithms perform poorly on latent fingerprints, as they are mostly based on assumptions that are only applicable for rolled/plain fingerprints.

In this work, we proposed the Adaptive Directional Total Variation (ADTV) model as an image decomposition scheme that facilitates effective latent fingerprint segmentation and enhancement. Based on the classical Total-Variation model, the proposed ADTV model differentiates itself by integrating two unique features of fingerprints, scale and orientation, into the model formulation. The proposed model has the ability to decompose a single latent image into two layers and locate the essential latent area for feature matching. The two spatially varying parameters of the model, scale and orientation, are adaptively chosen according to the background noise level and textural orientation, and effectively separate the latent fingerprint from structured noise in the background. It was shown by experimental results that the proposed ADTV scheme provides

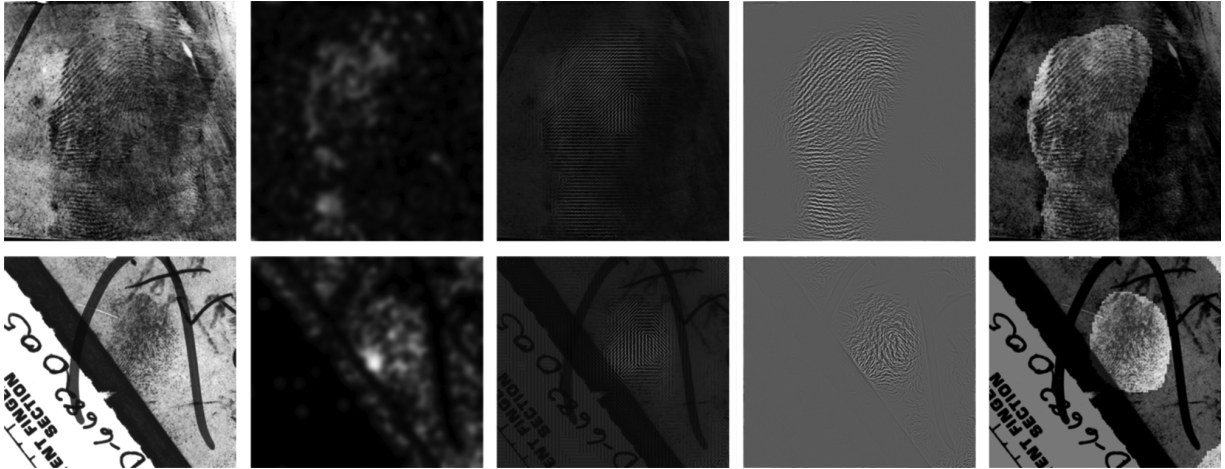


Fig. 14. Experimental results of two latent fingerprints with *bad* quality (from left to right): original image f , scale parameter $\lambda(x)$, orientation vector $\vec{a}(x)$, texture output v , and the final segmentation result.

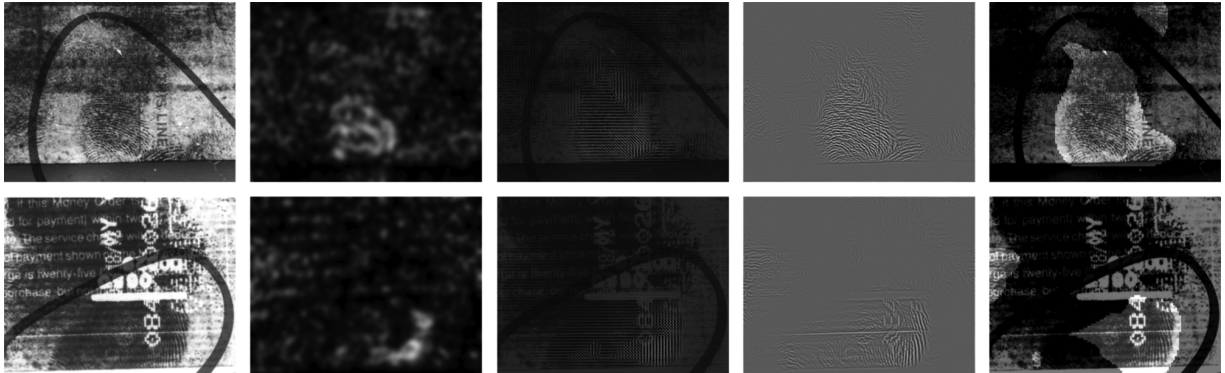


Fig. 15. Experimental results of two latent fingerprints with *ugly* quality (from left to right): original image f , scale parameter $\lambda(x)$, orientation vector $\vec{a}(x)$, texture output v , and the final segmentation result.

effective segmentation and enhancement. The improvements in feature detection accuracy and latent matching further justifies the effectiveness of the proposed scheme.

The proposed ADTV scheme can be viewed as a preprocessing technique in automatic latent fingerprint recognition. It also has a strong potential to be applied to other applications, especially for processing images with oriented textures. This study can be further extended along the following directions:

- 1) The effectiveness of the proposed scheme is related to the accuracy of orientation estimation. When the estimated orientation is unreliable, fingerprint patterns may not be fully extracted to texture layer v , leading to poor segmentation and enhancement results. In addition, the positions of singular points were not taken into consideration by the proposed model. Additional detection and processing techniques can be introduced for handling regions surrounding the singular points.
- 2) Some structured noise may have very similar characteristics as fingerprint patterns and cannot be blocked from the texture layer. For example, parallel straight lines have high coherency similar to fingerprints and could be extracted to the texture layer as well. Adding a preprocessing step to remove this type of structure noise may be a possible solution.
- 3) The proposed ADTV method is incapable of handling regions with overlapped fingerprints, as our model for-

mulation is designed to identify regions with coherent orientations along one single direction. To handle images with overlapped fingerprints, some sophisticated local analysis has to be conducted [7] and integrated into the model formulation.

ACKNOWLEDGMENT

The authors would like to thank Dr. X. Tang, Dr. L. Li, and other researchers at 3M Cogent Inc. for their support in data collection and researchers at Michigan State University for useful discussion.

REFERENCES

- [1] A. K. Jain and J. Feng, "Latent fingerprint matching," *IEEE Trans. Pattern Anal. Mach. Intell.*, vol. 33, no. 1, pp. 88–100, Jan. 2011.
- [2] B. M. Mehtre, N. N. Murthy, S. Kapoor, and B. Chatterjee, "Segmentation of fingerprint images using the directional image," *Pattern Recognit.*, vol. 20, no. 4, pp. 429–435, 1987.
- [3] B. Mehtre, "Segmentation of fingerprint images—a composite method," *Pattern Recognit.*, vol. 22, no. 4, pp. 381–385, 1989.
- [4] N. K. Ratha, S. Chen, and A. K. Jain, "Adaptive flow orientation-based feature extraction in fingerprint images," *Pattern Recognit.*, vol. 28, no. 11, pp. 1657–1672, 1995.
- [5] A. M. Bazen and S. H. Gerez, "Segmentation of fingerprint images," in *Proc. RISC 2001 Workshop on Circuits, Syst. and Signal Processing*, 2001, pp. 276–280.
- [6] J. Feng, S. Yoon, and A. K. Jain, "Latent fingerprint matching: Fusion of rolled and plain fingerprints," in *Proc. Third Int. Conf. Advances in Biometrics (ICB '09)*, Berlin, Heidelberg, 2009, pp. 695–704, Springer-Verlag.

- [7] F. Chen, J. Feng, A. K. Jain, J. Zhou, and J. Zhang, "Separating overlapped fingerprints," *IEEE Trans. Inf. Forensics Security*, vol. 6, no. 2, pp. 346–359, Jun. 2011.
- [8] S. Yoon, J. Feng, and A. K. Jain, "On latent fingerprint enhancement," in *Proc. Soc. Photo-Opt. Instrumentation Engineers (SPIE) Conf. Series*, Apr. 2010, vol. 7667.
- [9] S. Karimi-Ashtiani and C. C. J. Kuo, "A robust technique for latent fingerprint image segmentation and enhancement," in *Proc. IEEE Int. Conf. Image Processing*, 2008, pp. 1492–1495.
- [10] N. Short, M. Hsiao, A. Abbott, and E. Fox, "Latent fingerprint segmentation using ridge template correlation," in *Proc. IEEE Int. Conf. Imaging for Crime Detection and Prevention*, London, U.K., 2011.
- [11] H. Choi, M. Boaventura, I. Boaventura, and A. Jain, "Automatic segmentation of latent fingerprints," in *Proc. IEEE Fifth Int. Conf. Biometrics: Theory, Applicat. and Syst. (BTAS 2012)*, Sep. 2012, pp. 303–310.
- [12] W. Yin, D. Goldfarb, and S. Osher, "The total variation regularized ℓ_1 model for multiscale decomposition," *Multis. Model. Simul.*, vol. 6, pp. 190–211, 2006.
- [13] J.-F. Aujol, G. Gilboa, T. Chan, and S. Osher, "Structure-texture image decomposition-modeling, algorithms, and parameter selection," *Int. J. Comput. Vis.*, vol. 67, no. 1, pp. 111–136, Apr. 2006.
- [14] T. Chan and S. Esedoglu, "Aspects of total variation regularized ℓ_1 function approximation," *SIAM J. Appl. Math.*, vol. 65, pp. 1817–1837, 2004.
- [15] T. Chen, W. Yin, X. S. Zhou, D. Comaniciu, and T. S. Huang, "Total variation models for variable lighting face recognition," *IEEE Trans. Pattern Anal. Mach. Intell.*, vol. 28, no. 9, pp. 1519–1524, Sep. 2006.
- [16] J. Zhang, R. Lai, and C.-C. Kuo, "Latent fingerprint segmentation with adaptive total variation model," in *Proc. 5th IAPR Int. Conf. Biometrics (ICB 2012)*, 1, 2012, pp. 189–195.
- [17] J. Zhang, R. Lai, and C.-C. Kuo, "Latent fingerprint detection and segmentation with a directional total variation model," in *Proc. 19th IEEE Int. Conf. Image Processing (ICIP 2012)*, Oct. 3, 2012, vol. 30, pp. 1145–1148.
- [18] H. Fleyeh, D. Jomaa, and M. Dougherty, "Segmentation of low quality fingerprint images," in *Proc. Int. Conf. Multimedia Computing and Inform. Technol. (MCIT-2010)*, Mar. 2–4, 2010.
- [19] Z. Shi, Y. Wang, J. Qi, and K. Xu, "A new segmentation algorithm for low quality fingerprint image," in *Proc. IEEE Comput. Soc. Third Int. Conf. Image and Graph. (ICIG '04)*, Washington, DC, USA, 2004, pp. 314–317.
- [20] L. I. Rudin, S. Osher, and E. Fatemi, "Nonlinear total variation based noise removal algorithms," *Phys. D*, vol. 60, pp. 259–268, Nov. 1992.
- [21] T. Goldstein, X. Bresson, and S. Osher, "Geometric applications of the split Bregman method: Segmentation and surface reconstruction," *J. Sci. Comput.*, vol. 45, no. 1–3, 2009.
- [22] T. Goldstein and S. Osher, "The split Bregman method for ℓ_1 -regularized problems," *SIAM J. Imag. Sci.*, vol. 2, pp. 323–343, Apr. 2009.
- [23] S. Osher, M. Burger, D. Goldfarb, J. Xu, and W. Yin, "An iterative regularization method for total variation-based image restoration," *Multiscale Model. Simul.*, vol. 4, pp. 460–489, 2005.
- [24] C. Wu and X. Tai, "Augmented Lagrangian method, dual methods and split Bregman iterations for rof model, vectorial TV and higher order models," *SIAM J. Imag. Sci.*, vol. 3, pp. 300–339, 2010.
- [25] E. Esser, Applications of Lagrangian-based alternating direction methods and connections to split Bregman, UCLA CAM Rep. (09–31), 2009.
- [26] S. Setzer, "Split Bregman algorithm, Douglas-Rachford splitting and frame shrinkage," in *Proc. Second Int. Conf. Scale Space and Variational Methods in Comput. Vision (SSVM '09)*, Berlin, Heidelberg, 2009, pp. 464–476, Springer-Verlag.
- [27] J. Cai, S. Osher, and Z. Shen, "Split Bregman methods and frame based image restoration," *Multiscale Model. Simul.*, vol. 8, pp. 323–343, 2009.
- [28] R. Glowinski and P. L. Tallec, *Augmented Lagrangian and Operator-Splitting Methods in Nonlinear Mechanics*. Philadelphia, PA, USA: SIAM, 1989, vol. 9.
- [29] M. Hestenes, "Multiplier and gradient methods," *J. Optimizat. Theory Applicat.*, vol. 4, pp. 303–329, 1969.
- [30] X. Tai, J. Hahn, and G. Chung, "A fast algorithm for Euler's elastic model using augmented Lagrangian method," *SIAM J. Imag. Sci.*, vol. 4, pp. 313–344, 2011.
- [31] C. Wu, J. Zhang, and X.-C. Tai, "Augmented Lagrangian method for total variation restoration with non-quadratic fidelity," *Inverse Problems and Imaging IPI*, vol. 4, pp. 237–267, 2011.
- [32] L. Hong, Y. Wan, and A. Jain, "Fingerprint image enhancement: Algorithm and performance evaluation," *IEEE Trans. Pattern Anal. Mach. Intell.*, vol. 20, no. 8, pp. 777–789, Aug. 1998.
- [33] E. Zhu, J. Yin, C. Hu, and G. Zhang, "A systematic method for fingerprint ridge orientation estimation and image segmentation," *Pattern Recognit.*, vol. 39, no. 8, pp. 1452–1472, 2006.
- [34] A. Buades, T. M. Le, J.-M. Morel, and L. A. Vese, "Fast cartoon + texture image filters," *Trans. Img. Proc.*, vol. 19, pp. 1978–1986, Aug. 2010.
- [35] NIST Special Database 14, NIST Mated Fingerprint Card Pairs 2 (MFPC2) [Online]. Available: <http://www.nist.gov/srd/nistsd14.htm>
- [36] NIST Special Database SD27 [Online]. Available: <http://www.nist.gov/itl/iaid/ig/sd27a.cfm>
- [37] Latent Fingerprint Segmentation Result, Media Communications Lab [Online]. Available: http://viola.usc.edu/People/Jiangyang/TIFS-02732-2012_supplemental_materials.zip
- [38] Neurotechnology Inc., VeriFinger 2012 [Online]. Available: <http://www.neurotechnology.com>



Jiangyang Zhang received the B.S. degree in Telecommunications Engineering from Zhejiang University, China, in 2008. He has since started working on the Ph.D. degree at USC and joined the Media Communications Laboratory in January 2010. His main research interest lies in latent fingerprint processing and content-aware image/video resizing.



Rongjie Lai received the B.S. degree in mathematics from the University of Science and Technology of China, in 2003, the M.S. degree in mathematics from the Academy of Mathematics and System Science, Chinese Academy of Sciences, in 2006, and Ph.D. degree in applied mathematics from the University of California, Los Angeles, CA, USA, in 2010. He is currently an Assistant Professor (NTT) at the University of Southern California. His current research interests include computational differential geometry, calculus of variation and numerical PDE methods for image, and manifold processing.



C.-C. Jay Kuo (F'99) received the B.S. degree from the National Taiwan University, Taipei, Taiwan, in 1980, and the M.S. and Ph.D. degrees from the Massachusetts Institute of Technology, Cambridge, MA, USA, in 1985 and 1987, respectively, all in electrical engineering.

He is currently the Director of the Media Communications Laboratory and a Professor of electrical engineering, computer science, and mathematics at the University of Southern California, Los Angeles, CA, USA, and the President of the Asia-Pacific Signal and Information Processing Association (APSIPA). His current research interests include digital image/video analysis, multimedia data compression, and information forensics and security. He is a coauthor of about 210 journal papers, 850 conference papers, and 10 books.

Dr. Kuo is a fellow of the American Association for the Advancement of Science and the International Society for Optical Engineers.